

Probabilistic Traversability Model for Risk-Aware Motion Planning in Off-Road Environments

Xiaoyi Cai¹, Michael Everett¹, Lakshay Sharma¹, Philip R. Osteen², and Jonathan P. How¹

Abstract—A key challenge in off-road navigation is that even visually similar or semantically identical terrain may have substantially different traction properties. Existing work typically assumes a nominal or expected robot dynamical model for planning, which can lead to degraded performance if the assumed models are not realizable given the terrain properties. In contrast, this work introduces a new probabilistic representation of traversability as a distribution of parameters in the robot’s dynamical model that are conditioned on the terrain characteristics. This model is learned in a self-supervised manner by fitting a probability distribution over the parameters identified online, encoded as a neural network that takes terrain features as input. This work then presents two risk-aware planning algorithms that leverage the learned traversability model to plan risk-aware trajectories. Finally, a method for detecting unfamiliar terrain with respect to the training data is introduced based on a Gaussian Mixture Model fit to the latent space of the trained model. Experiments demonstrate that the proposed approach outperforms existing work that assumes nominal or expected robot dynamics in both success rate and completion time for representative navigation tasks. Furthermore, when the proposed approach is deployed in an unseen environment, excluding unfamiliar terrains during planning leads to improved success rate.

SUPPLEMENTARY MATERIAL

Video and GPU implementation of planners are available at https://github.com/mit-acl/mppi_numba.

I. INTRODUCTION

Progress in autonomous robot navigation has expanded the set of non-urban environments where robots can be deployed, such as mines, forests, oceans and Mars [1]–[4]. Unlike environments where safe and reliable navigation can be achieved by avoiding geometric hazards such as obstacles, navigation in forest-like environments poses unique challenges that still prevent systems from achieving good performance, because a purely geometric view of the world is not sufficient to identify non-geometric hazards (e.g., mud puddles, slippery surfaces) and geometric non-hazards (e.g., grass and foliage). To this end, recent approaches train semantic classifiers for camera images [5]–[9] or lidar pointclouds [10] in order to identify terrains or objects that could cause failures to the robotic platform. However, existing labeled datasets for off-road navigation have limited number of class labels such as “bush”, “grass”, and “tree” for vegetation without capturing the varying traversability within each class (e.g., [11], [12]),

or have limited transferability due to specificity to the vehicles that collected the data.

Instead of handcrafting cost functions based on geometric and semantic features, learning-based techniques are increasingly adopted to allow robots to learn traversability models by interacting with the environment autonomously or via human teleoperation. Although the terrain properties that affect traversability are different across applications, it is common that poor traversability leads to degraded performance or deviation from expected behaviors which, if measured reliably, can provide self-supervised learning signals without human annotation. For example, a robot can learn to correlate camera images and desired actions with likelihood of future collision and terrain bumpiness [13], terrain traction that affects achievable velocities [14], [15], or custom navigation costs [16]. Self-supervised learning can also be combined with unsupervised learning such that robots label observed data by discovering and clustering salient features in the input measurement that explain changes in task performance, e.g., via acoustic signals that reflect terrain bumpiness [17], [18]. Alternatively, the learning signals can be provided by human operators to teach terrain-dependent navigation behavior, such as the walking speed for quadrupeds [19].

While many techniques exist for traversability estimation, only a limited number of them explicitly account for the inherent uncertainty in the traversability model due to imperfect sensing and coarse semantic labels. In reality, visually similar or semantically identical terrains may lead to different outcomes, which makes using the expected traversability values inadequate to capture the risk of obtaining poor performance. For example, whether a robot gets stuck in tall grass could be a bi-modal distribution, but the mean of distribution suggests the robot can pass through with degraded performance. Furthermore, such uncertainty is typically fixed but unknown before the robot experiences it as opposed to being noise-like. Existing techniques like [13], [20] are risk-aware by predicting the probability of undesirable events such as collisions or the conditional value at risk (CVaR [21]) of the objective. In [15], the feasible speed distribution is learned and CVaR of the speed distribution is used in the objective to improve success rate. However, these methods all assume that the nominal or expected dynamics hold under different terrain conditions which, if untrue, makes the computed cost not representative of the true task performance. Therefore, capturing the uncertainty in robot dynamics (tightly coupled with the uncertainty in objective) is a crucial step towards mitigating the risk of obtaining poor performance.

To address these issues, we propose a new representation

¹Massachusetts Institute of Technology, Cambridge, MA 02139, USA.
 {xyc, mfe, lakshays, jhow}@mit.edu.

²DEVCOM Army Research Laboratory, Adelphi, MD 20783, USA.
 philip.r.osteen.civ@army.mil.

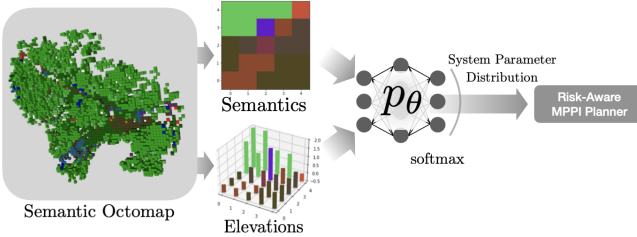


Fig. 1: Proposed pipeline for learning probabilistic traversability model and risk-aware motion planning. As the robot interacts with the environment, it incrementally builds a semantic octomap [22] while collecting terrain features and measurement of relevant system parameters to train a probabilistic traversability model in a self-supervised fashion. This model allows the proposed planner to compute risk-aware trajectories.

of traversability as the distribution of parameters in the robot’s dynamical model conditioned on terrain characteristics (as visualized in Fig 1). For concreteness, we focus the application scenarios around ground robots with unicycle dynamics whose linear and angular velocities are weighted by traction parameters. The traversability model can be learned in a self-supervised fashion and encoded as a neural network. In addition, we propose two novel planners that exploit the learned parameter distribution to plan risk-aware trajectories. These planners mitigate the risks that stem from either the stochastic dynamics or the downstream realization of the objectives, with different trade-off in performance and computational requirements. Lastly, as neural networks typically only interpolate within data observed during training, we design a detector for unfamiliar terrains based on a Gaussian Mixture Model (GMM) fit in the latent space of the trained neural network, which provides confidence scores that reflect how strongly a prediction is supported by training data. In summary, the contributions of this work are:

- A new representation of traversability as the distribution of parameters in the robot’s dynamical model conditioned on both geometric and semantic terrain features;
- Two novel planners based on Model Predictive Path Integral (MPPI [23]) control that use the terrain-dependent stochastic dynamics to plan trajectories that mitigate risks in either *dynamics* or *objective*, outperforming methods that assume nominal or expected dynamics;
- A GMM-based detector for unfamiliar terrains that improves success rate when the proposed pipeline is deployed in an unseen environment during training.

II. RELATED WORK

This section describes how the proposed work addresses key challenges in the field of off-road navigation, broadly categorized by methods for traversability representations, planning, and neural network uncertainty estimation.

A. Representations of Traversability

Traversability representation is a key component of off-road navigation algorithms; a more complete summary of various approaches is provided in [15], including representations based on proprioceptive measurements [24], [25], geometric features [1], [26]–[28] and combination of geometric

and semantic features [10], [29], [30]. WayFast [14] is a more recent approach, similar to this work, that proposes to represent traversability by learning traction coefficients for a unicycle model from terrain perception data. Another recent work [2] represents traversability as the probability of a quadruped robot to stabilize itself on uneven terrain, based on 3D occupancy data of the terrain. In [19], speed and gait policies are learned based on terrain semantics and human demonstrations; these policies provide a novel interpretation of the terrain’s traversability and can be used by the robot’s motor control policy. A key limitation, however, is that these point estimates of traversability do not capture the inherent variability in vehicle dynamics on similar-looking terrains. Instead, our approach represents traversability as a *distribution of parameters* in the robot’s dynamical model.

B. Planning with Terrain-Dependent Stochastic Dynamics

After learning a terrain-dependent stochastic dynamics model, a further challenge exists in incorporating this model into the planner. Despite capturing various types of uncertainties, many planners in this domain still assume a nominal or expected dynamics model such as [15], [20], [30]. Alternatively, our work is inspired by [31], which proposed a general framework for optimizing the CVaR of objectives for dynamical systems with uncertainties in dynamics, parameters and initial conditions by taking extra samples from sources of uncertainty. Adapting this method to off-road navigation, we propose a map representation to store learned distribution for the uncertain parameters that can be easily queried and sampled for long horizon planning. Moreover, to reduce computation of taking extra sampling, we propose to capture the worst-case impact of uncertain parameters via the CVaR of system parameters (applicable to commonly used ground vehicles) and use the worst-case parameters in the dynamics without the need to take extra samples.

C. Uncertainty Estimation for Neural Networks

In addition to capturing uncertainty in vehicle’s system parameters such as traction, it is important to estimate when the learned model is unfamiliar with a particular input example (e.g., from a terrain class that was not seen much in training, or from a substantially different environment). There are numerous techniques for estimating neural network uncertainty in classification or regression tasks, such as those based on Monte Carlo dropout [32], bootstrapping [33], or evidential learning [34], [35]. Some of these techniques have also been integrated into frameworks for planning under uncertainty [36], [37]. Although dropout and bootstrapping are standard approaches, the derived uncertainty score may not directly reflect how similar a query data is to the training data. Evidential learning attempts to provide epistemic uncertainty due to lack of data, but good uncertainty estimates require proper calibration by tuning the weights for a multi-objective loss function. This work instead proposes to estimate uncertainty to novel inputs via a generative model (i.e., GMM) built from the trained neural network’s latent

space, where the generative model can provide likelihood scores based on observed training data explicitly.

III. TRAVERSABILITY REPRESENTATION

Robot failures in the wild can be expensive in terms of time and money, so it is desirable for a planner to be *risk-aware*, where the planner should reduce the likelihood of worst-case failures. However, achieving risk-awareness relies on *uncertainty-awareness*, i.e., the planner knows the distribution of relevant random variables that impact performance. As a robot's dynamics depend on terrain, it's crucial to model the terrain-dependent uncertainty of robot dynamics in order to act proactively for risk minimization. Therefore, we propose a new representation of traversability as the terrain-dependent distribution for the system parameters. Using system identification techniques, a time sequence of system parameters can be obtained online as the robot interacts with the environment, which provides the learning signal for a neural network to model the terrain-vehicle interaction.

A. Terrain-Dependent Distribution over System Parameters

Denote the set of system parameters as $\Psi \subseteq \mathbb{R}^q$ and the set of possible observations about a terrain patch as \mathcal{O} , where $q > 0$ is the dimension of the parameter space. We can define traversability of the terrain as the conditional distribution

$$p_\theta(\psi | \mathbf{o}) : \Psi \times \mathcal{O} \rightarrow \mathbb{R}, \quad (1)$$

where $p_\theta \in \mathbf{P}_{\Psi|\mathcal{O}}$ is the set of all possible distribution for system parameters conditioned on terrain observation, $\psi \in \Psi$ is the system parameter vector, $\mathbf{o} \in \mathcal{O}$ is the observation about the terrain, and p_θ is a probability distribution parameterized by θ , which in practice can be learned by a neural network. Note that we do not restrict the form of the probability distribution so that rich traversability properties of the terrain can be modeled (e.g., the bimodal distribution of vegetation, as considered in Sec. V-D and Fig. 4).

In order to facilitate long-horizon planning, we represent traversability in a map such that the system parameters can be easily queried based on system states. Denoting the parameter distribution map as \mathbf{M} that belongs to the set of all possible maps \mathcal{M} , we also define a look-up function $\mathcal{S} : \mathcal{M} \times \mathbf{X} \rightarrow \mathbf{P}_\Psi$ such that a parameter distribution $p \in \mathbf{P}_\Psi$ can be queried as $p(\cdot) = \tilde{p}(\cdot | \mathbf{o}_x) = \mathcal{S}(\mathbf{M}, \mathbf{x})$ based on system state $\mathbf{x} \in \mathbf{X}$ and associated terrain observations \mathbf{o}_x . In practice, safety checks should be implemented to handle out-of-bound queries or queries in locations without any predicted distributions due to lack of measurement.

B. GMM-Based Detector for Unfamiliar Terrains

The traversability model is trained on a diverse set of experiences on different terrains. However, some terrain classes may have limited quantity in the training set, and real deployments of the system are likely to encounter scenarios outside the training distribution. In this work, we use a generative model based on GMM in the latent space of a trained neural network, in order to have a probabilistic model for assigning likelihood for any input query based on its distance to clusters of training data in the latent space.

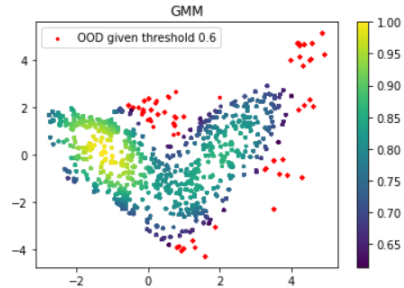


Fig. 2: Visualization of GMM-based detector for unfamiliar terrains, where query data with low confidence score will be discarded. In this example, data with score less than 0.6 are marked in red as out-of-distribution (“OOD”), where other data are colored based on normalized scores.

After training the neural network to model terrain traversability, we apply principal component analysis (PCA) to the latent space, and fit a GMM for the entire training dataset in the reduced latent space. An example of a trained model is shown in Fig. 2, where PCA is applied to reduce dimension to 2 and the GMM has 2 clusters for simplicity. The confidence score is based on the log-likelihood of the query data, normalized between the maximum and minimum log-likelihood observed in training data. During deployment, normalized log-likelihood less than the threshold $p^{\text{thres}} \in [0, 1]$ are discarded. Intuitively, the further away a query data lies from the cluster centers, the less similarity the query data shares with the training data. This detector can be used to exclude unfamiliar terrains, thereby improving the success rate of missions as demonstrated in Sec. V-E.

IV. PLANNING WITH A DISTRIBUTION MAP OF DYNAMICS PARAMETERS

We adopt the MPPI controller proposed in [23, Algorithm 2] for minimum time planning. MPPI is an information theoretic model predictive control (MPC) algorithm that tries to approximate the mean of the optimal control distribution via weighted samples of a Gaussian proposal distribution in order to minimize the KL-divergence between the two. This approach is attractive because it is derivative-free and works with general cost functions and dynamics. Next, we adapt the notation in [23] to our problem involving uncertain parameters of the dynamics model.

A. Dynamics Model

Consider the discrete time stochastic system:

$$\mathbf{x}_{t+1} = F(\mathbf{x}_t, \mathbf{v}_t, \psi_t), \quad (2)$$

where $\mathbf{x}_t \in \mathbf{X} \subseteq \mathbb{R}^n$ is the state vector, $\mathbf{v}_t \in \mathbb{R}^m \sim \mathcal{N}(\mathbf{u}_t, \Sigma)$ is the noisy realization of the nominal control input $\mathbf{u}_t \in \mathbb{R}^m$, and system parameter $\psi_t \in \Psi$ is sampled from a ground truth distribution $p_t^* \in \mathbf{P}_{\Psi|\mathcal{O}}$ which is typically unknown. As we don't have access to the ground truth distribution for the system parameters, we can approximate it with a neural network parameterized by θ .

During deployment, the learned conditional distribution $p_\theta \in \mathbf{P}_{\Psi|\mathcal{O}}$ is converted into a look-up map $\mathbf{M}_\theta \in \mathcal{M}$ to produce the parameter distribution $p_{\theta, \mathbf{x}_t} = \mathcal{S}(\mathbf{M}_\theta, \mathbf{x}_t)$ that is already conditioned on the terrain features at state \mathbf{x}_t .

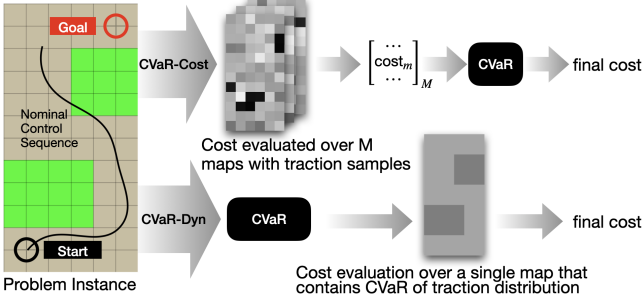


Fig. 3: Qualitative difference between the two proposed risk-aware cost functions CVaR-Cost and CVaR-Dyn. For every control sequence, the CVaR-Cost planner samples M terrain traction parameters to obtain a vector of costs. Subsequently, a final cost is obtained as the CVaR of these costs in the worst α -quantile. On the other hand, the CVaR-Dyn planner extracts a single traction map whose values are the CVaR of the traction parameters in the worst α -quantile, thus avoiding the need to sample M traction maps.

Given the initial condition \mathbf{x}_0 , a sequence of input $\mathbf{v}_{0:T-1}$ we obtain a sequence of system parameters $\psi_{0:T-1}$ and the state trajectory $\mathbf{x}_{0:T}$ according to the dynamics (2):

$$p_{\theta, \mathbf{x}_t}(\cdot) = \mathcal{S}(\mathbf{M}_\theta, \mathbf{x}_t), \quad (3)$$

$$\psi_t \sim p_{\theta, \mathbf{x}_t}(\cdot), \quad (4)$$

$$\mathbf{x}_{t+1} = F(\mathbf{x}_t, \mathbf{v}_t, \psi_t). \quad (5)$$

The cost function C , evaluated for trajectory $\mathbf{x}_{0:T}$, yields the scalar cost $c \in \mathbb{R}$, which can be formulated as

$$c := C(\mathbf{x}_{0:T}) = \phi(\mathbf{x}_T) + \sum_{t=0}^{T-1} q(\mathbf{x}_t), \quad (6)$$

where $\phi(\mathbf{x}_T)$ and $q(\mathbf{x}_t)$ are the terminal cost and the stage cost, respectively. Note that c is a random variable that depends on the other two random variables \mathbf{v}_t and ψ_t . As the MPPI algorithm was designed to handle only the uncertainty due to \mathbf{v}_t , we need to take extra samples in order to account for the randomness introduced by the uncertain system parameters ψ_t as discussed in the Sec. IV-B.

At each time t and given the nominal control sequence $\mathbf{u}_{t:t+T}$, MPPI estimates the mean of the optimal control distribution as the weighted sum of $N > 0$ control rollouts that are sampled from $\mathcal{N}(\mathbf{u}_\tau, \Sigma)$ for all $t \leq \tau \leq t+T$. The weight of each rollout indexed by $n \in \{1, \dots, N\}$ is an exponentiated version of (6), denoted c^n , evaluated along the induced state trajectory. The algorithm runs in an receding horizon fashion, where the nominal control sequence $\mathbf{u}_{t+1:t+T+1}$ in the next round is set to be newest estimate of the mean of the optimal control distribution.

B. Risk-Aware Cost Function for MPPI

In order to account for the risk of obtaining high cost due to the uncertain system parameters ψ_t , we propose to optimize two modified versions of the cost function (6). A high-level schematic showing the core ideas behind the two cost functions can be found in Fig. 3.

1) *Worst-Case Expected Cost (CVaR_Cost):* Given every sampled control sequence $\mathbf{v}_{0:T-1}^n$ where $n \in \{1, \dots, N\}$, we sample from the parameter distribution map \mathbf{M}_θ in order to obtain $M > 0$ maps that contain samples of the system

parameter $\psi_{h,w}^m$ for every map cell $x_{h,w}$ indexed by height h and width w in \mathbf{M}_θ . As a result, for every control sequence, we obtain a set of cost values $\{c^{n,m}\}_{m=1}^M$ that represent the effect of random system parameters. In order to remain risk-aware to the worst realizations of the costs, our proposed cost function is

$$c^n := C^{\text{risk_cost}}(\mathbf{x}_{0:T}) = \text{getCVaR}(\{c^{n,m}\}_{m=1}^M, \alpha) \quad (7)$$

where $\text{getCVaR}(\cdot, \cdot)$ computes worst-case expectation of cost values and $\alpha \in (0, 1]$ determines the quantile over which to compute the expectation. Since the objective is being minimized, the worst-case corresponds to the right-side tail of the cost distribution. For example, if $\alpha = 0.1$, the mean of the worst 10% of the cost values are used. Note that this approach is inspired by [31], but we additionally have to handle terrain-dependent distribution of parameters.

2) Worst-Case Expected System Parameters (CVaR_Dyn):

The procedure of sampling large number of maps that contain system parameters can be efficiently parallelized on GPUs, but the computation can still grow prohibitively for high-dimensional systems. Therefore, we propose a second cost design that allows us to capture the risk of obtaining high cost due to uncertain parameters by using the worst-case expectation of the robot dynamics (instead of using just the mean estimates like [14]), which eliminate the need to sample from of parameter distribution. We focus our discussion around the unicycle robot dynamics introduced in Sec. V-A for concreteness. Note that this approach may not generalize to more complex systems where the impact of system parameters on the performance is less clear.

The system parameters for the unicycle are $\mu, \nu \in [0, 1]$ which represent terrain traction, i.e., the ratio between commanded velocity and realizable velocity based on the terrain. In order to navigate reliably and quickly in the forest, it is desirable to have perfect traction $\mu = \nu = 1$. Therefore, given the parameter distribution for $\psi = [\mu, \nu]^\top$, the worst-case expectation in traction can be computed:

$$\psi_t^{\text{risk}} = \text{getCVaRSystemParams}(p_{\theta, \mathbf{x}_t}(\cdot), \alpha) \quad (8)$$

where $\text{getCVaRSystemParams}(\cdot, \cdot)$ computes expectation for the left-side tail (near 0) of the traction parameters, where $\alpha \in (0, 1]$ specifies desired quantile. As ψ_t^{risk} summarizes the worst-case expected traction values, we can avoid sampling $M > 0$ times from the parameter distribution maps. Therefore, for each control sequence \mathbf{v}_t^n :

$$\begin{aligned} \mathbf{x}_{t+1}^{\text{risk_dyn}} &= F(\mathbf{x}_t^{\text{risk_dyn}}, \mathbf{v}_t^n, \psi_t^{\text{risk}}), \\ c^n &:= C(\mathbf{x}_{0:T}^{\text{risk_dyn}}) = \phi(\mathbf{x}_T^{\text{risk_dyn}}) + \sum_{t=0}^{T-1} q(\mathbf{x}_t^{\text{risk_dyn}}). \end{aligned}$$

When $\alpha = 1$, the expected values of the traction parameters are used, which is equivalent to the approach in [14]. However, as the results in Sec. V-D show for a go-to-goal task, planning with the worst-case expected traction can lead to higher success rate and shorter time-to-goal.

V. SIMULATION RESULTS

A. Robot Dynamics

Consider the following discrete-time unicycle model:

$$\mathbf{x}_{t+1}^{\text{Unicycle}} = \begin{bmatrix} p_{t+1}^x \\ p_{t+1}^y \\ \theta_{t+1} \end{bmatrix} = \begin{bmatrix} p_t^x \\ p_t^y \\ \theta_t \end{bmatrix} + \Delta \cdot \begin{bmatrix} \mu \cdot v_t \cdot \cos(\theta_t) \\ \mu \cdot v_t \cdot \sin(\theta_t) \\ \nu \cdot \omega_t \end{bmatrix}, \quad (9)$$

where the state $\mathbf{x}_t^{\text{Unicycle}}$ consists of X position p_t^x , Y position p_t^y , and the yaw orientation θ_t . The model propagates with time interval of $\Delta > 0$ based on the control $\mathbf{u}_t^{\text{Unicycle}} = [v_t, w_t]^\top$, and the system parameters $\psi^{\text{Unicycle}} = [\mu, \nu]^\top$ represent terrain traction where $\mu, \nu \in [0, 1]$ whose range goes from no traction to perfect traction.

B. Cost Function

The cost function follows the min-time formulation used in [15] but has an additional distance-based term in the stage cost. Let $\mathbb{1}^{\text{done}}(\mathbf{x}_{0:t})$ be an indicator function that returns 1 when any state \mathbf{x}_τ has reached the goal at position \mathbf{p}^{goal} for $0 \leq \tau \leq T$, and returns 0 otherwise. Next, we define the terminal cost $\phi(\mathbf{x}_T)$ and the stage cost $q(\mathbf{x}_t)$ as

$$\phi(\mathbf{x}_T) = \frac{\|\mathbf{p}^{\text{goal}} - \mathbf{p}_T\|}{s^{\text{default}}} (1 - \mathbb{1}^{\text{done}}(\mathbf{x}_{0:T})), \quad (10)$$

$$q(\mathbf{x}_t) = \Delta (1 - \mathbb{1}^{\text{done}}(\mathbf{x}_{0:t})) + w^{\text{dist}} \cdot \|\mathbf{p}^{\text{goal}} - \mathbf{p}_t\|, \quad (11)$$

where s^{default} is the default speed for estimating time-to-go at the end of the rollout, Δ is the sampling duration, and $w^{\text{dist}} > 0$ is the weight for penalizing distance from the goal. Note that once the robot reaches the goal, the rollout stops accumulating stage costs to encourage faster arrival.

C. Implementation Details

A computer with Intel Core i9 CPU and Nvidia GeForce RTX 3070 GPU is used for the simulations, where majority of the computation happens on the GPU. The MPPI planners run in a receding horizon fashion with 100 time steps (10 s at 10 Hz). The max linear and angular speeds are capped at 3 m/s and π rad/s, and the noise standard deviations for the control signals are 2 m/s and 2 rad/s. The number of control rollouts is 1024 and the number of sampled traction maps is 1024 (only applicable for the CVaR_Cost planner). We use probability mass functions with 20 uniform bins to approximate the parameter distribution. The CVaR_Cost planner is the most expensive to compute, but it is able to re-plan at 15 Hz while sampling new control actions and maps with dimension of 200×200 . Planners that do not sample traction maps can be executed at over 50 Hz.

D. Navigation on Randomly Generated Semantic Maps

We show that the proposed planners achieve better performance than ones that do not leverage the full traction distribution through a grid world scenario, where ‘‘dirt’’ and ‘‘vegetation’’ cells have known traction distributions, as shown in Fig. 4. Vegetation patches are randomly spawned in increasing probabilities at the center of the arena, and a robot may experience significant slow-down for certain vegetation cells due to vegetation’s bi-modal distribution.

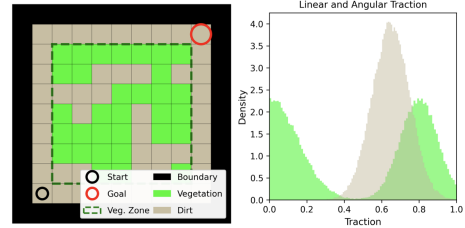


Fig. 4: The simulation environment where a robot has to move from start to goal as fast as possible within the bounded arena. Linear and angular traction parameters share the same distribution for simplicity. Vegetation terrain patches are randomly sampled at the center.

Overall, we sample 40 different semantic maps and 5 random realizations of traction parameters for every semantic map. The traction parameters are drawn before starting each trial and remain fixed (i.e., ‘‘fixed unknown’’). The benchmark results can be found in Fig. 5, where we compare the two proposed methods with existing methods, namely WayFAST [14] that uses the expected traction and the technique in [15] that assumes nominal dynamics while adjusting the time cost with the CVaR of linear traction. The takeaway is that the proposed methods outperform the two existing ones by using knowledge about the full distribution of traction parameters (being uncertainty-aware) in order to reduce the likelihood of high cost due to the bimodal traction in vegetation (being risk-aware). Notably, although the CVaR_Dyn planner does not sample from the entire parameter distribution, it achieves similar performance to the CVaR_Cost planner when α is set sufficiently low. The poor performance of the CVaR_Cost planner can be attributed to the difficulty of estimating CVaR from samples in general when α is low. However, the CVaR_Dyn planner makes conservative assumption about the dynamics, so it does not out-perform CVaR_Cost in achieving low time-to-goal.

E. Simulated Terrain Traversability from Real-World Data

In this section, we demonstrate that the proposed GMM-based detector for novel input can be used, by excluding unfamiliar terrains during planning, to improve the mission success rate when a trained traversability model is deployed in an environment not seen during training. To this end, we prepared two real-world datasets and deployed the proposed pipeline (see Fig. 1) to generate training data and test environment. The two datasets were collected from different forests by a Clearpath Husky robot equipped with an Ouster lidar, forward facing RealSense camera and a Microstrain IMU. The sensors were used to provide odometry estimates and build the semantic octomap. Based on the history of robot’s trajectory, commanded velocities, and the semantic octomap, we are able to obtain a time series of terrain traction and terrain features for training the traversability model.

The generated semantic and elevation maps for the training environment are visualized in Fig. 6a, where the data collection trajectory has been overlaid on the semantic map. Overall fewer than 10 minutes of data are used to train the traversability model, which will be deployed in a simulated test environment whose semantic top-down view is shown

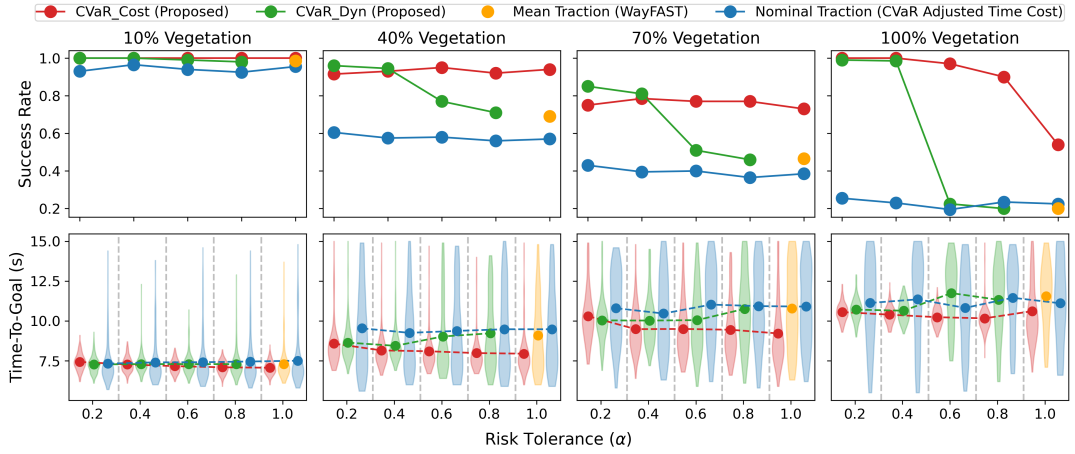


Fig. 5: Results comparing the proposed methods (CVaR_Cost and CVaR_Dyn in Sec. IV-B) against existing methods based on the expected traction (WayFAST [14]) and method that assumes nominal traction but adjusts the time cost based on CVaR of linear traction [15]. Overall, the CVaR_Cost planner always maintains better success rate and time-to-goal than WayFAST and the method using nominal traction. As the risk tolerance increases, the CVaR_Cost planner becomes more optimistic and achieves lower time-to-goal. When the risk tolerance is sufficiently low (e.g., $\alpha = 0.2$), the second proposed planner CVaR_Dyn achieves similar or better success rate and time-to-goal compared to the CVaR_Cost planner. Intuitively, CVaR_Dyn uses the worst-case dynamics for rollouts, effectively treating the vegetation terrain types as obstacles and avoiding them.

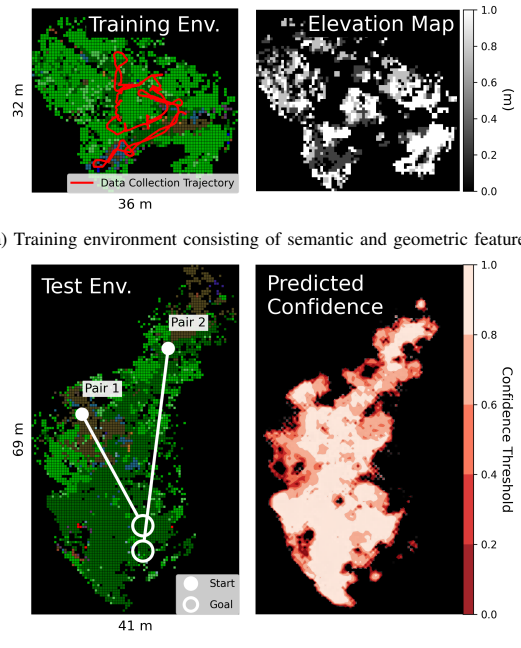


Fig. 6: Illustration of the two environments used for training and testing the proposed pipeline and the GMM-based detector for unfamiliar terrains.

in Fig. 6b. In order to deploy the trained model in the a second unseen environment in simulation, we train a second traversability model using the test dataset in order to provide a proxy to the ground truth traversability models. This model is only used as part of the simulation and is not used by the planner. For each of the two pairs of start-goal positions visualized in Fig. 6b, 10 trials are executed with different ground truth traction maps for a given choice of confidence score threshold from 0 to 1. The result of deploying the proposed CVaR_Cost planner with risk tolerance $\alpha = 1.0$ that samples both the control sequences and traction maps can be shown in Fig. 7. Overall, as the threshold confidence

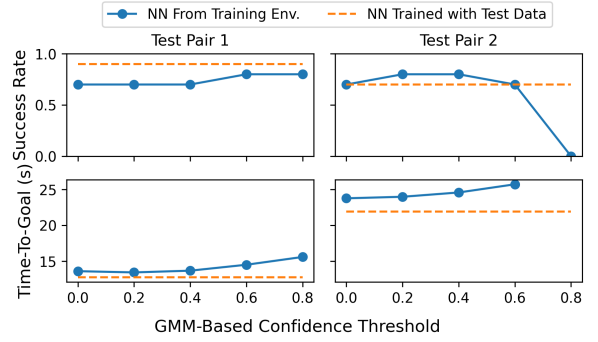


Fig. 7: Impact of GMM-based detector on mission performance.

level increases, more unfamiliar terrains are excluded from the planning problem which leads to increased time-to-goals. However, the success rate increases because the robot can avoid regions where the network's prediction may be significantly different from the ground truth. However, the confidence threshold has to be carefully chosen, because it may lead to infeasibility as there's no feasible path between start and goal, as is the case for Test Pair 2.

VI. CONCLUSION & FUTURE WORK

This work proposed a probabilistic traversability model that can be trained in a self-supervised fashion for system parameters in robot dynamics. Using this model, the proposed planners were shown to achieve better success rate and time-to-goal for representative navigation tasks, compared to techniques that assumed nominal or expected dynamics. Furthermore, when deployed in unseen environments, the proposed GMM-based detector for unfamiliar terrains led to improved success rate. Future work includes adjusting risk-tolerance of planner online based on terrain, unsupervised terrain feature extraction, and running hardware experiments.

ACKNOWLEDGMENT

Research was sponsored by ARL W911NF-21-2-0150.

REFERENCES

[1] D. D. Fan, K. Otsu, Y. Kubo, A. Dixit, J. Burdick, and A.-A. Agha-Mohammadi, “Step: Stochastic traversability evaluation and planning for risk-aware off-road navigation,” in *Robotics: Science and Systems*. RSS Foundation, 2021, pp. 1–21.

[2] J. Frey, D. Hoeller, S. Khattak, and M. Hutter, “Locomotion policy guided traversability learning using volumetric representations of complex environments,” *arXiv preprint arXiv:2203.15854*, 2022.

[3] A. A. Pereira, J. Binney, G. A. Hollinger, and G. S. Sukhatme, “Risk-aware path planning for autonomous underwater vehicles using predictive ocean models,” *Journal of Field Robotics*, vol. 30, no. 5, pp. 741–762, 2013.

[4] M. Massari, G. Giardini, and F. Bernelli-Zazzera, “Autonomous navigation system for planetary exploration rover based on artificial potential fields,” in *Proceedings of Dynamics and Control of Systems and Structures in Space (DCSS) 6th Conference*, 2004, pp. 153–162.

[5] A. Valada, G. Oliveira, T. Brox, and W. Burgard, “Deep multispectral semantic scene understanding of forested environments using multimodal fusion,” in *International Symposium on Experimental Robotics (ISER)*, 2016.

[6] A. Valada, J. Vertens, A. Dhall, and W. Burgard, “Adapnet: Adaptive semantic segmentation in adverse environmental conditions,” in *2017 IEEE International Conference on Robotics and Automation (ICRA)*. IEEE, 2017, pp. 4644–4651.

[7] Z. Chen, D. Pushp, and L. Liu, “Cali: Coarse-to-fine alignments based unsupervised domain adaptation of traversability prediction for deployable autonomous navigation,” *arXiv preprint arXiv:2204.09617*, 2022.

[8] T. Guan, D. Kothandaraman, R. Chandra, A. J. Sathyamoorthy, K. Weerakoon, and D. Manocha, “Ga-nav: Efficient terrain segmentation for robot navigation in unstructured outdoor environments,” *IEEE Robotics and Automation Letters*, vol. 7, no. 3, pp. 8138–8145, 2022.

[9] T. Guan, Z. He, R. Song, D. Manocha, and L. Zhang, “Tns: Terrain traversability mapping and navigation system for autonomous excavators,” *arXiv preprint arXiv:2109.06250*, 2021.

[10] A. Shaban, X. Meng, J. Lee, B. Boots, and D. Fox, “Semantic terrain classification for off-road autonomous driving,” in *Conference on Robot Learning*. PMLR, 2022, pp. 619–629.

[11] M. Wigness, S. Eum, J. G. Rogers, D. Han, and H. Kwon, “A rugged dataset for autonomous navigation and visual perception in unstructured outdoor environments,” in *International Conference on Intelligent Robots and Systems (IROS)*, 2019.

[12] P. Jiang, P. Osteen, M. Wigness, and S. Saripalli, “Rellis-3d dataset: Data, benchmarks and analysis,” in *2021 IEEE International Conference on Robotics and Automation (ICRA)*. IEEE, 2021, pp. 1110–1116.

[13] G. Kahn, P. Abbeel, and S. Levine, “Badgr: An autonomous self-supervised learning-based navigation system,” *IEEE Robotics and Automation Letters*, vol. 6, no. 2, pp. 1312–1319, 2021.

[14] M. V. Gasparino, A. N. Sivakumar, Y. Liu, A. E. B. Velasquez, V. A. H. Higuti, J. Rogers, H. Tran, and G. Chowdhary, “Wayfast: Navigation with predictive traversability in the field,” *IEEE Robotics and Automation Letters*, vol. 7, no. 4, pp. 10651–10658, 2022.

[15] X. Cai, M. Everett, J. Fink, and J. P. How, “Risk-aware off-road navigation via a learned speed distribution map,” *arXiv preprint arXiv:2203.13429*, 2022.

[16] A. J. Sathyamoorthy, K. Weerakoon, T. Guan, J. Liang, and D. Manocha, “Terrapn: Unstructured terrain navigation through online self-supervised learning,” *arXiv preprint arXiv:2202.12873*, 2022.

[17] J. Zürn, W. Burgard, and A. Valada, “Self-supervised visual terrain classification from unsupervised acoustic feature learning,” *IEEE Transactions on Robotics*, vol. 37, no. 2, pp. 466–481, 2020.

[18] X. Yao, J. Zhang, and J. Oh, “Rca: Ride comfort-aware visual navigation via self-supervised learning,” *arXiv preprint arXiv:2207.14460*, 2022.

[19] Y. Yang, X. Meng, W. Yu, T. Zhang, J. Tan, and B. Boots, “Learning semantics-aware locomotion skills from human demonstration,” *arXiv preprint arXiv:2206.13631*, 2022.

[20] D. D. Fan, A.-A. Agha-Mohammadi, and E. A. Theodorou, “Learning risk-aware costmaps for traversability in challenging environments,” *IEEE Robotics and Automation Letters*, vol. 7, no. 1, pp. 279–286, 2021.

[21] A. Majumdar and M. Pavone, “How should a robot assess risk? towards an axiomatic theory of risk in robotics,” in *Robotics Research*. Springer, 2020, pp. 75–84.

[22] A. Asgharivaskasi and N. Atanasov, “Active bayesian multi-class mapping from range and semantic segmentation observations,” in *2021 IEEE International Conference on Robotics and Automation (ICRA)*. IEEE, 2021, pp. 1–7.

[23] G. Williams, N. Wagener, B. Goldfain, P. Drews, J. M. Rehg, B. Boots, and E. A. Theodorou, “Information theoretic mpc for model-based reinforcement learning,” in *2017 IEEE International Conference on Robotics and Automation (ICRA)*. IEEE, 2017, pp. 1714–1721.

[24] F. G. Oliveira, A. A. Neto, D. Howard, P. Borges, M. F. Campos, and D. G. Macharet, “Three-dimensional mapping with augmented navigation cost through deep learning,” *Journal of Intelligent & Robotic Systems*, vol. 101, no. 3, pp. 1–21, 2021.

[25] S. Otte, C. Weiss, T. Scherer, and A. Zell, “Recurrent neural networks for fast and robust vibration-based ground classification on mobile robots,” in *2016 IEEE International Conference on Robotics and Automation (ICRA)*. IEEE, 2016, pp. 5603–5608.

[26] J. Larson, M. Trivedi, and M. Bruch, “Off-road terrain traversability analysis and hazard avoidance for ugv’s,” California University San Diego, Dept. of Electrical Engineering, Tech. Rep., 2011.

[27] T. Overbye and S. Saripalli, “Fast local planning and mapping in unknown off-road terrain,” in *2020 IEEE International Conference on Robotics and Automation (ICRA)*. IEEE, 2020, pp. 5912–5918.

[28] ———, “G-vom: A GPU accelerated voxel off-road mapping system,” *arXiv preprint arXiv:2109.13176*, 2021.

[29] T. Guan, Z. He, D. Manocha, and L. Zhang, “Ttm: Terrain traversability mapping for autonomous excavator navigation in unstructured environments,” *arXiv preprint arXiv:2109.06250*, 2021.

[30] Y. Tan, N. Virani, B. Good, S. Gray, M. Yousefhussien, Z. Yang, K. Angeliu, N. Abate, and S. Sen, “Risk-aware autonomous navigation,” in *Artificial Intelligence and Machine Learning for Multi-Domain Operations Applications III*, vol. 11746. International Society for Optics and Photonics, 2021, p. 117461D.

[31] Z. Wang, O. So, K. Lee, and E. A. Theodorou, “Adaptive risk sensitive model predictive control with stochastic search,” in *Learning for Dynamics and Control*. PMLR, 2021, pp. 510–522.

[32] Y. Gal and Z. Ghahramani, “Dropout as a bayesian approximation: Representing model uncertainty in deep learning,” in *international conference on machine learning*. PMLR, 2016, pp. 1050–1059.

[33] I. Osband, C. Blundell, A. Pritzel, and B. Van Roy, “Deep exploration via bootstrapped dqn,” *Advances in neural information processing systems*, vol. 29, 2016.

[34] M. Sensoy, L. Kaplan, and M. Kandemir, “Evidential deep learning to quantify classification uncertainty,” *Advances in neural information processing systems*, vol. 31, 2018.

[35] A. Amini, W. Schwarting, A. Soleimany, and D. Rus, “Deep evidential regression,” *Advances in Neural Information Processing Systems*, vol. 33, pp. 14927–14937, 2020.

[36] G. Kahn, A. Villaflor, V. Pong, P. Abbeel, and S. Levine, “Uncertainty-aware reinforcement learning for collision avoidance,” *arXiv preprint arXiv:1702.01182*, 2017.

[37] B. Lütjens, M. Everett, and J. P. How, “Safe reinforcement learning with model uncertainty estimates,” in *2019 International Conference on Robotics and Automation (ICRA)*. IEEE, 2019, pp. 8662–8668.